Earth Surface Processes and Landforms
Earth Surf. Process. Landforms **29**, 907–926 (2004)
Published online in Wiley InterScience (www.interscience.wiley.com). DOI: 10.1002/esp.1083

HYPSOMETRY OF GLACIATED LANDSCAPES

SIMON H. BROCKLEHURST[1]* AND KELIN X. WHIPPLE[2]

[1] *Cooperative Institute for Research in Environmental Sciences and Department of Geological Sciences, University of Colorado, Boulder, CO 80309, USA*

[2] *Department of Earth, Atmospheric and Planetary Sciences, Massachusetts Institute of Technology, Cambridge, MA 02139, USA*

Received 12 December 2002; Revised 19 December 2003; Accepted 5 February 2004

ABSTRACT

Hypsometry (frequency distribution of elevations) is often used to characterize landscape morphology, traditionally in the context of the degree of fluvial dissection. Recently, the hypsometry of glaciated regions has been used to infer how rates of glacial erosion compare with tectonic uplift rates. However, many factors other than tectonics can also exert a major influence on the hypsometry of a glaciated landscape, resulting in a wide variety of hypsometries. Using examples from the eastern Sierra Nevada, California, the western Sangre de Cristo Range, Colorado, and the Ben Ohau Range, New Zealand, we demonstrate that, all else being equal, the hypsometries of neighbouring basins can indicate the relative degree of glacial modification in each. A selection of drainage basins from the Rocky Mountains shows that the position of the equilibrium line altitude (ELA) within the drainage basin relief is a dominant variable in determining the hypsometry of a glaciated basin. This is a non-linear effect: once the ELA falls to some critical level, the glaciers scour deeply below the ELA, causing a noticeably different hypsometry. The hypsometry of an arbitrary region encompassing many drainage basins can disguise the variation present in the hypsometries, and thus landforms, of the individual basins. Unique local circumstances, such as the presence of a mountain icefield (Waiho Basin, Southern Alps), substantial hanging valleys (Avalanche Creek, Glacier National Park), a narrow outlet canyon (Sawmill Creek, Sierra Nevada), and isolated geologic structures (Baker Creek, Sierra Nevada), can have a major impact on the hypsometry of an individual basin. Copyright © 2004 John Wiley & Sons, Ltd.

KEY WORDS: hypsometry; glacial erosion; glaciated landscapes

INTRODUCTION

Potential interactions between climate change and tectonic processes have sparked much interest in recent years, as authors have debated whether tectonic processes can influence global climate or indeed if climate change can drive tectonic processes (e.g. Molnar and England, 1990; Raymo and Ruddiman, 1992; Brozovic *et al*., 1997; Small and Anderson, 1998; Whipple *et al*., 1999). In order to evaluate the role of climatic cooling during the late Cenozoic, it is particularly important to understand the role of glaciers in shaping the evolving landscape, because most active mountain ranges in temperate latitudes have been at least partially glaciated (e.g. Brozovic *et al*., 1997; Braun *et al*., 1999; MacGregor *et al*., 2000; Merrand and Hallet, 2000; Tomkin and Braun, 2002; Brocklehurst and Whipple, 2002). Hypsometry (frequency distribution of elevations) is an important tool in the study of glaciated landscapes using digital topographic data. Brozovic *et al*. (1997) used the hypsometry of glaciated landscapes in the Nanga Parbat region to examine their response to varying tectonic uplift rates, and Montgomery *et al*. (2001) used hypsometry to argue for changes in the relative importance of fluvial, glacial, and tectonic processes along the Andes. However, our preliminary studies (Brocklehurst and Whipple, 2000) suggested that hypsometry can be non-unique, and other factors, such as the degree of glaciation, or the presence of an icefield, can also cause considerable variation in the hypsometries of glaciated landscapes. This paper explores the variety in the hypsometry of glaciated landscapes in the absence of dramatic tectonic activity (i.e. considering only rock uplift rates of less than *c*. 1 mm/yr).

Hypsometry describes the distribution of elevations within an area of interest, and has several different guises. Typically, 'hypsometry' refers to a frequency distribution of elevations. The hypsometric curve then represents

* Correspondence to: S. H. Brocklehurst, Department of Earth Sciences, The University of Manchester, Manchester, M13 9PL, UK.
E-mail: shb@man.ac.uk

the fraction of basin area below a given height, usually reported in non-dimensional terms by normalizing the elevations relative to the total elevation range in the area of interest. The hypsometric integral is the area under this normalized curve, which by definition must lie in the range 0 to 1, and typically varies between *c*. 0·3 and *c*. 0·6 in fluvial landscapes. The region of interest is arbitrary, ranging from a single drainage basin (e.g. Strahler, 1952) to entire continents (e.g. Harrison *et al*., 1983). Hypsometry has classically been used in fluvial landscapes to differentiate erosional landforms at progressive stages in their evolution (Strahler, 1952; Schumm, 1956). Strahler (1952) asserted that the hypsometric integral decreases as a landscape 'matures' during post-orogenic topographic decay. Willgoose and Hancock (1998) showed that hypsometry is strongly dependent on channel network and catchment geometry, and is a scale-dependent descriptor of landforms, as fluvial processes become more dominant with respect to hillslopes in larger basins. Hurtrez *et al*. (1999) also reported that hypsometry is dependent on drainage area. Lifton and Chase (1992) demonstrated that lithology influences the hypsometric integral at smaller scales.

The hypsometry of glaciated landscapes has not been explored in such detail. Hypsometry places an important control on glacier mass balance (e.g. Small, 1995). When the equilibrium line altitude (ELA) moves as a result of climate change, the change in the extent of glaciated terrain depends on hypsometry. If a large portion of a region lies at an elevation similar to the ELA, small changes in ELA can significantly affect the proportion of surface area covered by glaciers. In addition to occupying, and eroding, a much larger area, larger glaciers will have a substantially higher ice discharge, and will modify the landscape much more significantly than their smaller counterparts. Furthermore, the faster accumulation area is lost during climate amelioration and ELA rise, the faster the glacier terminus must retreat (Small, 1995). Kirkbride and Matthews (1997) found that, in the Ben Ohau Range of New Zealand, increasing glacial influence is manifest in smoother, more concave long profiles and U-shaped cross-profiles, associated with a higher proportion of the land area at lower elevation. In terms of hypsometry, this puts a greater proportion of the landscape at lower elevations within the basin.

Recent studies have focused on interpreting the hypsometry of glaciated landscapes in terms of their response to tectonic activity. Brozovic *et al*. (1997) found that the hypsometries of glaciated landscapes around Nanga Parbat are independent of rock uplift rates, but are correlated with the snowline elevation, implying that glacial erosion rates can match uplift rates in actively deforming regions, and climate dominates landscape evolution. Montgomery *et al*. (2001) argued that hypsometry demonstrates the relative dominance of fluvial, glacial and tectonic processes in different regions of the Andes. They deduced that rivers dominate the northern Andean landscape, neither fluvial nor glacial erosion can compete with tectonics in the Altiplano, the dry central portion of the Andes, and glaciers dominate landscapes in the southern Andes, in spite of tectonic uplift. While we agree with the interpretations in this case, we caution that, in general, interpretations made from hypsometry can be non-unique. As we show here, other factors, such as varying degrees of glaciation and ELA position, can produce similar variations in hypsometry.

We carried out a comprehensive series of analyses to assess the influences of the degree of glaciation, the position of the ELA, and the selection of a drainage basin versus an arbitrary region, on the hypsometry of glaciated landscapes. We selected field sites in the western USA and the South Island of New Zealand in order to isolate each of these factors and assess the influence of each on hypsometry and thus landscape form. The effect of more rapid tectonic uplift rates on the hypsometry of glaciated mountain ranges is considered elsewhere (Brocklehurst and Whipple, in preparation).

MOTIVATION

Given that glaciated landforms are quite distinct from their fluvial counterparts (e.g. Sugden and John, 1976; Benn and Evans, 1998), it seems reasonable to infer that such differences will be reflected in the hypsometry of the two landscapes, with the degree of glacial modification of the landscape reflected in the hypsometry. Many authors argue that glacial erosion is focused at and above the ELA (e.g. Andrews, 1972; MacGregor *et al*., 2000). This follows from the assumption that erosion scales with ice velocity and, in MacGregor *et al*.'s (2000) study, basal water pressure fluctuations. In simple models both of these variables are at a maximum at the ELA, so as the ELA descends and then re-ascends during a glacial cycle, the zone of maximum erosion will sweep down, then back up, resulting in an eroded landscape focused above the lowest ELA. Thus it would follow that

the position of the ELA within the drainage basin of interest would have a major influence on the landscape. However, most simple models ignore flow convergence, and in valleys where two or more tributaries combine in the lower reaches, velocities can be at a maximum well below the contemporary ELA.

Recent work has examined large (i.e. multiple drainage basin), arbitrary regions of landscapes to deduce the relative importance of glacial and tectonic processes (Brozovic *et al*., 1997; Montgomery *et al*., 2001). However, given that no two drainage basins are exactly alike, it would seem that selecting arbitrary regions, while appropriate for regional-scale studies, might obscure some of the local details that would otherwise be visible in the hypsometry of individual basins. Glacial landscapes potentially harbour significant local variations in landforms caused, for instance, by icefields and hanging valleys.

Thus we sought to test the following four hypotheses, focusing on individual drainage basins, a natural unit for landscape analysis.

(i) Hypsometry is an effective indicator of long-term degree of glaciation.
(ii) The position of the ELA within the drainage basin relief has a significant influence on the hypsometry of a glaciated basin.
(iii) The hypsometry of large, arbitrary regions can mask the detail and variation shown by individual drainage basins.
(iv) Unique local circumstances, such as the presence of icefields and hanging valleys, can have a profound effect on the hypsometry.

METHODS

We employed two different methods for analysing hypsometry. The first method (e.g. Figure 2a–c) is a simple *histogram* of the frequencies in different elevation bins, for instance as employed by Brozovic *et al*. (1997). The chosen bin size is a compromise between not gaining enough information with too large a bin size, and obscuring the signal with scatter in the data with too small a bin size. In practice, we found a 100 m bin size most appropriate. Secondly, we generated a *hypsometric curve* (e.g. Figure 2d), normalized elevation plotted against normalized cumulative area (e.g. Strahler, 1952). The area under this curve, which by definition lies in the range 0 to 1, is the hypsometric integral, *HI*, estimated using:

$$HI = \frac{H_{mean} - H_{min}}{H_{max} - H_{min}} \tag{1}$$

where H_{max}, H_{mean}, and H_{min} are the maximum, mean and minimum elevations in the basin, respectively. Our analyses within the USA were carried out using 30 m digital elevation models (DEMs) from the USGS, whereas for the New Zealand examples we used a 50 m DEM from TerraLink.

To test hypothesis (i), we sought drainage basins within a short latitudinal range that exhibit varying degrees of glacial modification (determined independently from published geologic maps, our own field observations, and aerial photograph and topographic map interpretation), but with uniform lithology and tectonics. These criteria were satisfied in sections of the eastern Sierra Nevada, California (Figure 1a), the western Sangre de Cristo Range, southern Colorado (Figure 1b), and the eastern Ben Ohau Range, New Zealand (Figure 1c; Kirkbride and Matthews, 1997). On the regional scale, the section of the Sierra Nevada studied (Figure 1a) consists of homogeneous Cretaceous granodiorites and quartz monzonites (Moore, 1963, 1981; Bateman, 1965). Present-day tectonic activity is dominated by strike-slip motion on the Owens Valley Fault farther to the east, although the range-front normal fault system may still be active, contributing to fairly uniform uplift rates on the order of *c*. 0·2 mm/yr (Gillespie, 1982). The principal lithologies of the western side of the Sangre de Cristo Range (Figure 1b) are Palaeozoic sedimentary units and Precambrian metamorphic rocks (Johnson *et al*., 1987). Normal faulting slip rates along the range front in the region of interest have averaged around 0·1–0·2 mm/yr during the late Pleistocene (McCalpin, 1986, 1987), comparable to rates measured in the Sierra Nevada. The eastern side of the Ben Ohau Range (Figure 1c) is dominated by greywacke and argillaceous metasediments, with minor schist and localized volcanic rocks (Spörli and Lillie, 1974). Rock uplift rates inferred from fission

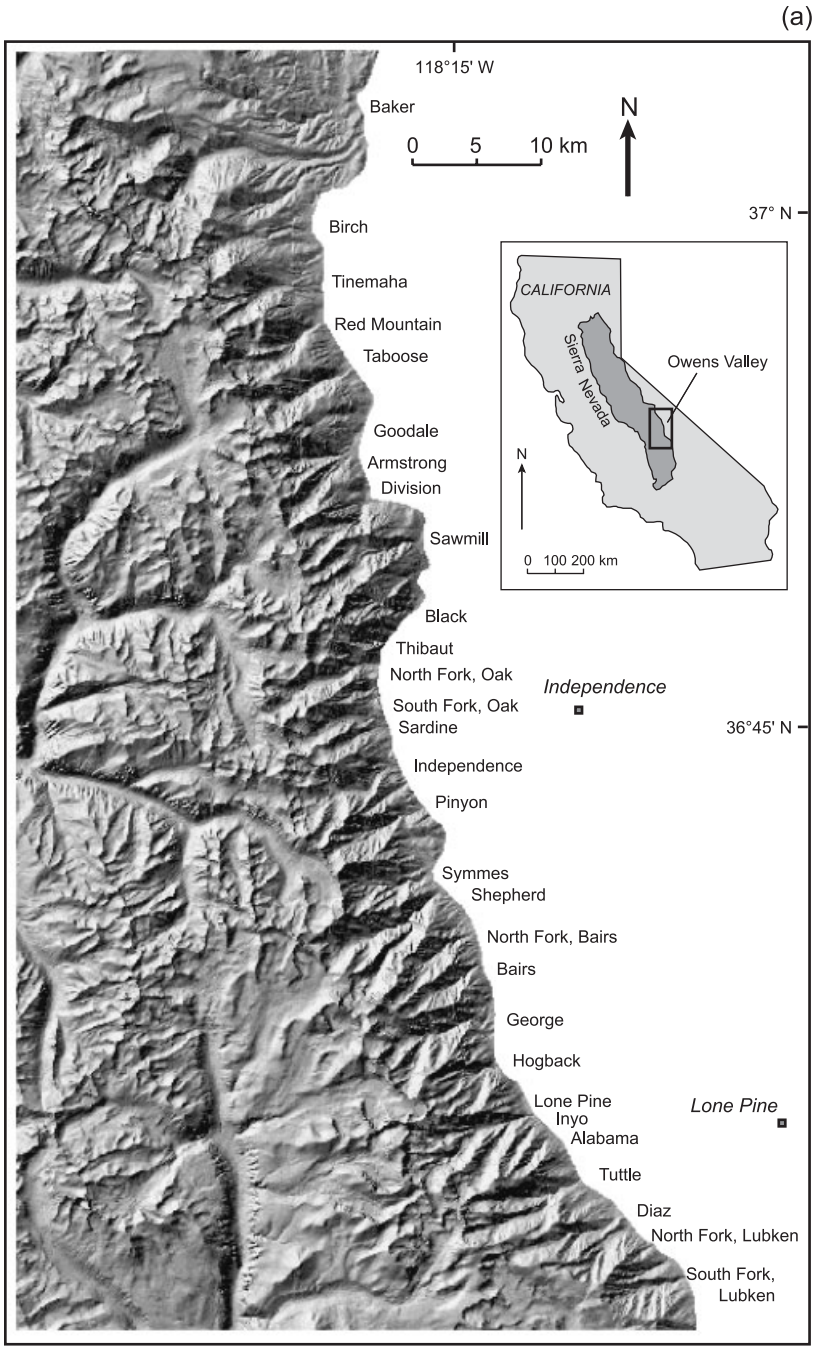

Figure 1. (a) Shaded relief map of drainage basins studied in the eastern Sierra Nevada, California. Location of study site shown in inset map. (b) Shaded relief map of drainage basins studied in the Sangre de Cristo Range, southern Colorado. Location of study site shown in inset map. (c) Shaded relief map of drainage basins studied in the Ben Ohau Range, South Island, New Zealand. Location of study site shown in inset map

track data of *c*. 0·8 mm/yr (Tippett and Kamp, 1995a, b) agree well with uplift rates of *c*. 1 mm/yr obtained from monitoring the range-bounding Ostler Fault Zone (Blick *et al*., 1989).

The eastern Sierra Nevada and western Sangre de Cristos exhibit a spectrum from basins essentially lacking any glacial modification through to what we here call 'fully glaciated' drainages, basins that at the last glacial

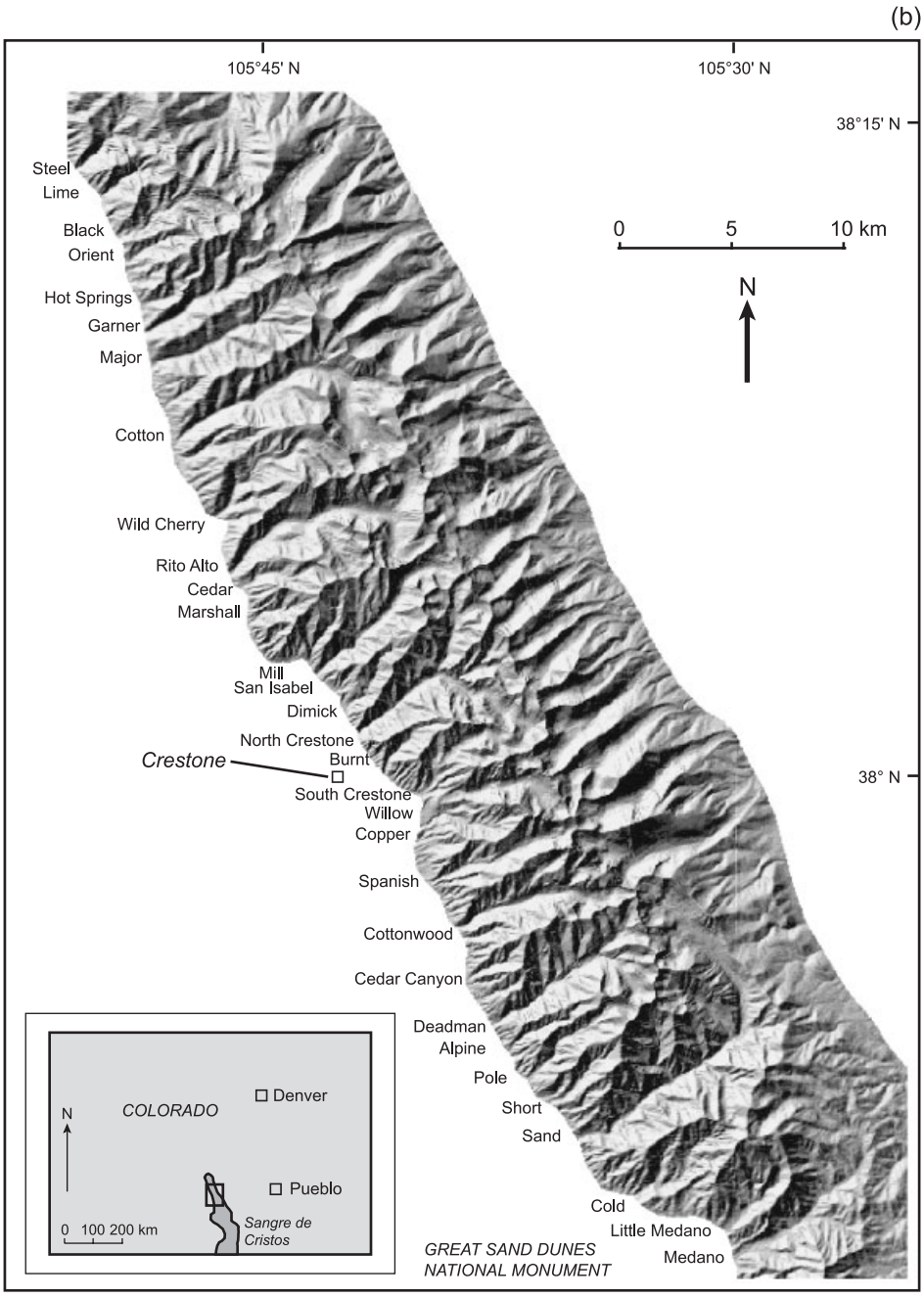

Figure 1. (*continued*)

maximum (LGM) contained glaciers extending to the range front. The extent of glaciation at the LGM in the Ben Ohau Range varied from small cirque glaciers at the southern end of the range to large tributary glaciers to the Tasman Glacier at the northern end of the range.

To test hypothesis (ii), we focused on 'fully glaciated' catchments in the Rocky Mountains, from the Sangre de Cristo Range in southern Colorado, the Bitterroot Range in southern Idaho, and Glacier National Park in northern Montana. From south to north, the mean Quaternary ELA steadily declines, both in absolute terms and also within the drainage basin relief of the catchments studied.

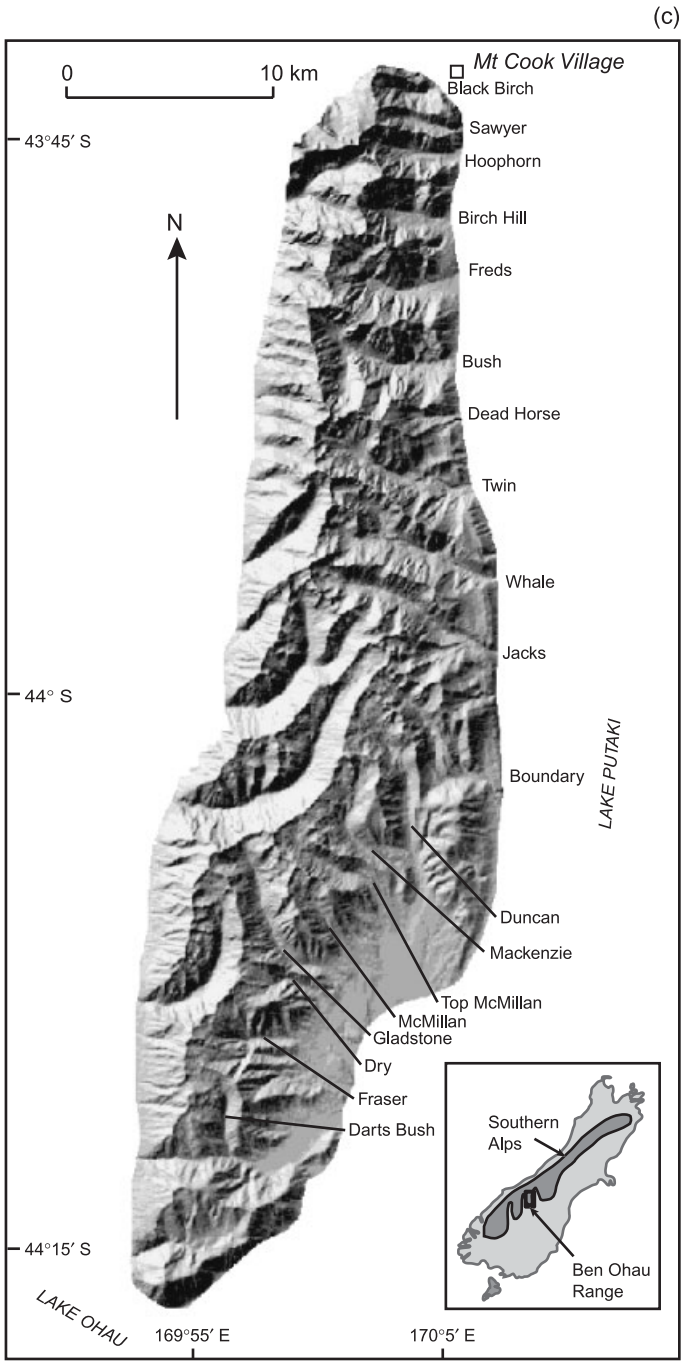

Figure 1. (*continued*)

To test hypothesis (iii), we compared drainage basin hypsometry with the hypsometry of arbitrary regions of the Sierra Nevada. We followed the same hypsometric methods summarized above, and compared the results with those from the individual drainage basins in the same region.

Finally, in order to evaluate hypothesis (iv), we examined the potentially extreme impacts of: (a) a mountain icefield, by looking at the hypsometry of basins draining the west side of Mt Cook in the Southern Alps of

New Zealand (Brocklehurst and Whipple, submitted); (b) prominent hanging valleys, in Glacier National Park; (c) narrow outlet canyons, in the eastern Sierra Nevada; and (d) local geologic structures, also in the eastern Sierra Nevada.

RESULTS

Hypsometry as an indicator of the degree of glaciation

Figure 2 illustrates hypsometry and hypsometric curves for 28 drainage basins on the eastern side of the Sierra Nevada (Brocklehurst and Whipple, 2002), with hyposmetric integrals given for Table I. We highlight three representative examples with bold lines, with the remaining basins shown with faint lines on the hypsometric curve plot (Figure 2d). In Figure 2a–c, the dashed grey lines illustrate the modern and LGM ELAs for each drainage basin taken from regional trends (Burbank, 1991). We took ELAs determined using the accumulation–area ratio method (AAR = 0·65) for mapped former glacier extents, rather than those derived from cirque floor elevations, since hypsometry is not independent of cirque floor elevations. (Note that by definition local LGM ELA must vary between non-glaciated and glaciated basins.) As shown, the regional ELA gradient is modest. Inyo Creek preserves no evidence of glacial occupation during the Quaternary. Hogback Creek developed a small glacier that never reached the range front. Lone Pine Creek supported a larger glacier that extended to the range front at the Last Glacial Maximum (LGM). There is a consistent pattern to the hypsometry as a function of the degree of glaciation across all of the drainages. Non-glaciated basins have a frequency distribution of elevations skewed towards lower elevations, and thus a low hypsometric integral. Moderate glaciation causes

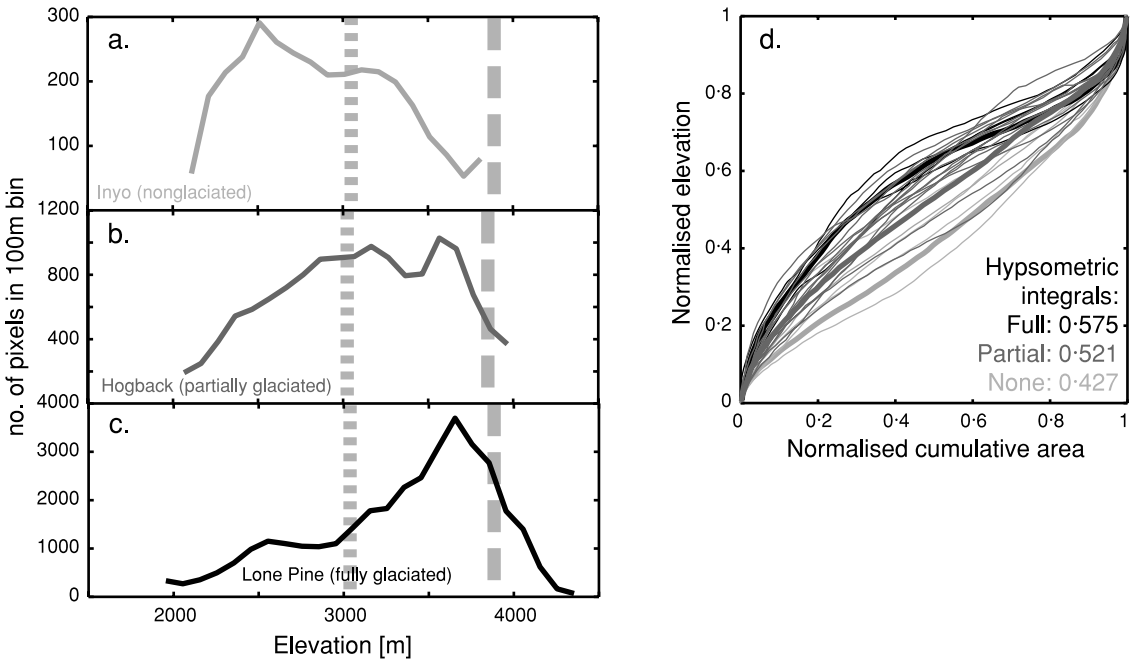

Figure 2. Hypsometry of the eastern Sierra Nevada. Modern (dashed) and Last Glacial Maximum (dotted) regional equilibrium line altitudes for the crest of the range from Burbank (1991). (a) Non-glaciated Inyo Creek. (b) Partially glaciated Hogback Creek. (c) Glaciated Lone Pine Creek. (d) Hypsometric curves and integrals (area under the hypsometric curve) for Inyo (light grey), Hogback (dark grey) and Lone Pine (black) Creeks (thick lines), and the remaining basins in the range following the same scheme (thin lines: light grey, non-glaciated; dark grey, partially glaciated; black, fully glaciated). The highlighted examples are representative of the hypsometric curves and integrals of non-glaciated, partially glaciated and glaciated basins respectively. Notice how increasing degree of glaciation causes a shift in the mode of the frequency distribution to higher elevations, corresponding to an increase in the hypsometric integral. This reflects the development of wide, flat cirque floors and flattening of the glacial valley longitudinal profile at high elevation (Brozovic *et al.*, 1997; Brocklehurst and Whipple, 2002)

Table I. Summary of Sierra Nevada hypsometry data. Basins listed in alphabetical order. Mean values for hypsometric integral are: non-glaciated, 0·46; minor glaciation, 0·52; moderate glaciation, 0·52; significant glaciation, 0·57; full glaciation, 0·58. Minor, moderate and significant glaciation are collectively referred to in the text as partial glaciation

Basin	Degree of glaciation	Hypsometric integral
Alabama	None	0·452
Black	None	0·532
Inyo	None	0·427
Pinyon	None	0·485
South Fork, Lubken	None	0·396
Symmes	None	0·491
Diaz	Minor	0·531
Division	Minor	0·592
Thibaut	Minor	0·443
Bairs	Moderate	0·478
Goodale	Moderate	0·607
Hogback	Moderate	0·521
North Fork, Bairs	Moderate	0·448
North Fork, Lubken	Moderate	0·532
Red Mountain	Moderate	0·532
Armstrong	Significant	0·533
George	Significant	0·589
North Fork, Oak	Significant	0·590
Sardine	Significant	0·581
Sawmill	Significant	0·590
Shepherd	Significant	0·552
Taboose	Significant	0·569
Tuttle	Significant	0·542
Birch	Full	0·567
Independence	Full	0·563
Lone Pine	Full	0·575
South Fork, Oak	Full	0·589
Tinemaha	Full	0·624

a more even frequency distribution and an intermediate hypsometric integral. Further glacial modification results in both the peak in the frequency distribution becoming skewed towards higher elevations, and higher hypsometric integrals. Figure 3 shows the same plots for 31 basins draining the western side of the Sangre de Cristos, again highlighting three representative examples, with hypsometric integrals given in Table II. As before, Figure 3a–c illustrate, with dashed grey lines, modern and LGM ELAs from regional trends (Richmond, 1965). Here ELAs were determined using a terminus-to-headwall altitude ratio (THAR) of 0·5, again providing an independent test of the influence of ELA position on topography. Marshall Creek preserves no significant evidence of glacial modification. The glacier in Wild Cherry Creek never reached the range front, whilst the Rito Alto Creek glacier did at the LGM. The pattern observed in the hypsometry is much the same as in the Sierra Nevada (Figure 2), although the relief of the Sangre de Cristo range is about half that of the Sierra Nevada.

In comparison with the Sierra Nevada, the Ben Ohau Range has a much stronger gradient in ELA (both current and LGM, using an AAR of 0·6), varying from close to the outlet elevation of the basins in the northern part of the range, to near the crest of the range in the south, as shown by the dashed grey lines in Figure 4a–c (Porter, 1975). Hypsometry data are summarized in Table III. The highlighted, representative examples from the Ben Ohau Range show a trend relating to glacial impact that is the opposite of that seen in the eastern Sierra Nevada and the western Sangre de Cristo Range. During the last major glaciation, McMillan River had a small cirque glacier at its head, Whale River developed a small valley glacier, and Black Birch River had a glacier that extended beyond the range front as a tributary to the Tasman Glacier. In this case, the least glacial modification results in a frequency distribution skewed towards high elevation (reflecting a modest cirque

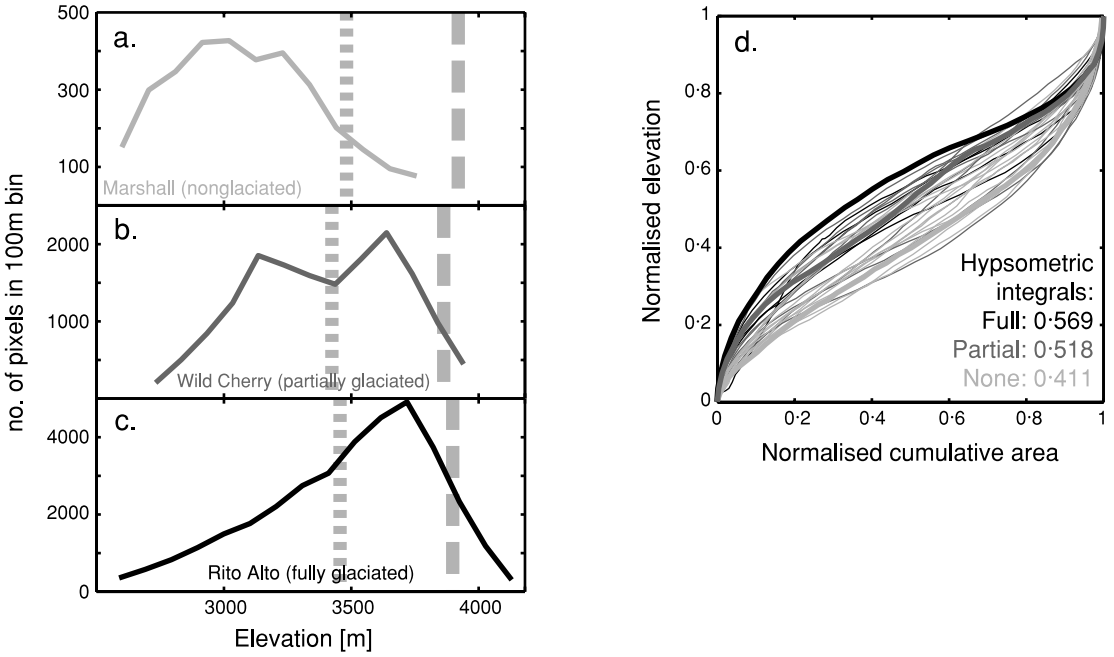

Figure 3. Hypsometry of the Sangre de Cristo Range. Modern (dashed) and LGM (dotted) regional ELAs for the crest of the range from Richmond (1965). (a) Non-glaciated Steel Creek. (b) Partially glaciated Wild Cherry Creek. (c) Glaciated Rito Alto Creek. (d) Hypsometric curves and integrals for Steel (light grey), Wild Cherry (dark grey) and Rito Alto (black) Creeks (thick lines), and the remaining basins in the range following the same scheme (thin lines). The highlighted examples are representative of the hypsometric curves and integrals of non-glaciated, partially glaciated and glaciated basins respectively. As in the Sierra Nevada, an increasing degree of glaciation causes a shift in the mode of the frequency distribution to higher elevations, along with a decrease in hypsometric integral, reflecting the development of the wide, flat-bottomed glacial trough

glacier), and increasing glaciation shifts the mode of the frequency distribution to successively lower elevations, correspondingly decreasing the hypsometric integral. This is consistent with what Kirkbride and Matthews (1997) report, namely that 'increasing glacial influence is manifest as smoother, more deeply concave long profiles and U-shaped cross-profiles associated with a higher proportion of the land at lower elevation'.

This result suggests that there is a key difference in the impact of glacial erosion on the eastern Sierra Nevada and western Sangre de Cristos compared with the Ben Ohau Range. We suggest that this is due to the position of the mean Quaternary ELA within the total relief of the mountain range. In general, glaciated landscapes predominantly reflect the glaciers that would have been present under a mean Quaternary ELA (Porter, 1989). If the ELA is proportionally lower within the basin, it seems logical to infer that a higher proportion of the basin will have been subjected to major glacial modification, development of wide valley floors and U-shaped cross-sections, etc., and that this will be reflected in the hypsometry. This hypothesis is tested in the next section.

Influence of ELA position on hypsometry

We have attempted to quantify the relative ELA position within the total elevation range of the basin using the following formula:

$$ELA_{norm} = \frac{ELA_{Qm} - z_0}{z_{max} - z_0} \tag{2}$$

Here ELA_{norm} is the relative mean Quaternary ELA position, ELA_{Qm} is the mean Quaternary ELA, defined as midway between the modern and LGM ELAs (Porter, 1989), z_0 is the outlet elevation for the basin, and z_{max} is the maximum elevation in the basin. As defined, a value of 1 for ELA_{norm} indicates a mean Quaternary ELA at the highest point in the basin, and a value of 0 indicates a mean Quaternary ELA at the outlet. Here we are

Table II. Summary of Sangre de Cristos hypsometry data. Basins listed in alphabetical order. Mean values for hypsometric integral are: non-glaciated, 0·46; partially glaciated, 0·50; fully glaciated, 0·52

Basin	Degree of glaciation	Hypsometric integral
Alpine	None	0·449
Burnt	None	0·437
Cedar Canyon	None	0·502
Cold	None	0·401
Copper	None	0·395
Dimick	None	0·423
Hot Springs	None	0·463
Lime	None	0·500
Little Medano	None	0·471
Marshall	None	0·411
Mill	None	0·523
Orient	None	0·447
Short	None	0·439
Steel	None	0·510
Cedar	Partial	0·533
Cottonwood	Partial	0·516
Deadman	Partial	0·542
Garner	Partial	0·432
Major	Partial	0·432
Medano	Partial	0·388
North Crestone	Partial	0·532
Pole	Partial	0·479
Sand	Partial	0·511
San Isabel	Partial	0·558
Spanish	Partial	0·503
Wild Cherry	Partial	0·518
Black	Full	0·469
Cotton	Full	0·538
Rito Alto	Full	0·569
South Crestone	Full	0·483
Willow	Full	0·521

interested in variations in hypsometry as ELA_{norm} declines, i.e. as the ELA becomes proportionally lower in the basin. Mean values for ELA_{norm} are 0·67, 0·64 and 0·57 for the Sangre de Cristo Range, Bitterroot Range, and Glacier National Park respectively. Figure 5 compares the hypsometries of fully glaciated basins in these three ranges, highlighting Rito Alto Creek in the Sangre de Cristos, Sawtooth Creek in the Bitterroots, and Walton Creek in Glacier National Park, with hypsometric integrals given in Table IV. Again these are representative examples of each of the study areas. In each case the LGM glaciers extended at least to the range front, but as indicated by the thick grey lines (and the differing ELA_{norm} values), the ELA position within the relief of the basin varies markedly. The result of lowering the ELA within the relief of the range is to shift the major peak in hypsometry to lower elevations, and, consequently, to reduce the hypsometric integral. It is noteworthy that the shift in the peak in the frequency distribution is far greater than the shift in ELA.

Comparing arbitrary regions and drainage basins

Figure 6 illustrates the effects of selecting a larger, arbitrary section of topography from the eastern Sierra Nevada, in comparison with representative drainage basins within this area. The selected portion runs from Independence Creek in the north to Lone Pine Creek in the south, and as such encompasses these two fully glaciated basins, five partially glaciated basins (Shepherd, North Fork Bairs, Bairs, George, and Hogback) and four non-glaciated basins (Pinyon, Symmes, Inyo, and Alabama – see Figure 1a). The result of combining these basins into a larger unit is a hypsometry that looks much like a partially glaciated basin, both in the frequency

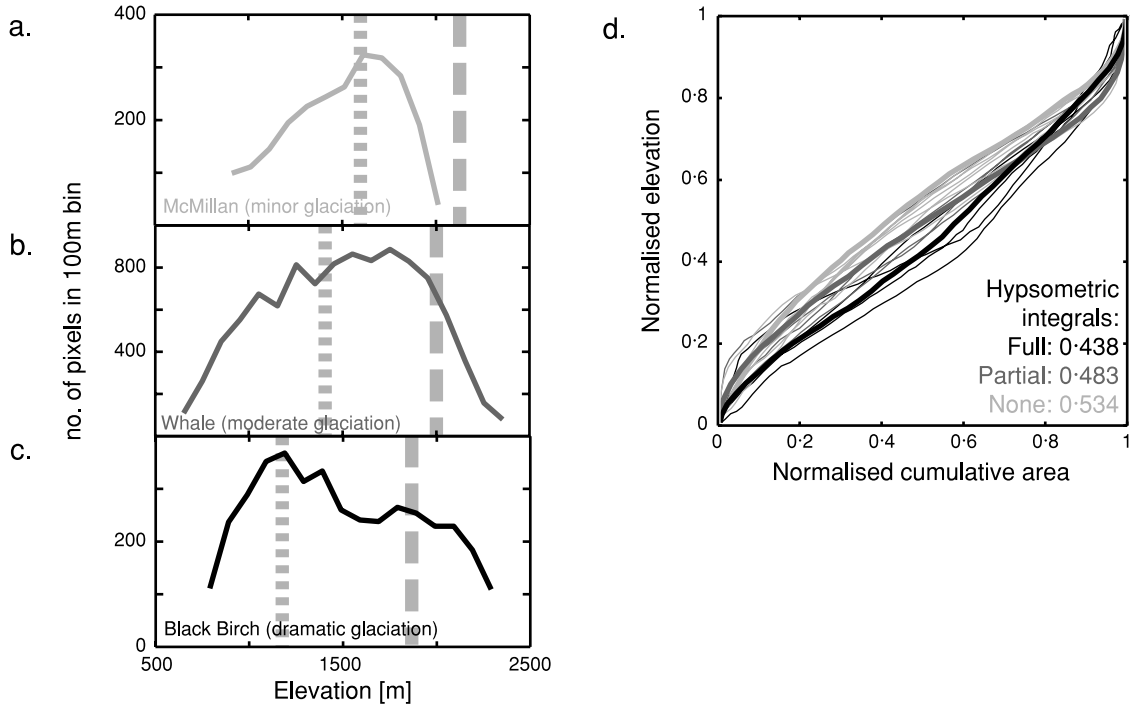

Figure 4. Hypsometry of the Ben Ohau Range. Modern (dashed, grey) and LGM (dotted, grey) regional ELAs for the crest of the range from Porter (1975). (a) Non-glaciated McMillan River. (b) Partially glaciated Whale River. (c) Glaciated Black Birch River. (d) Hypsometric curves and integrals for McMillan (light grey), Whale (dark grey) and Black Birch (black) Rivers (thick lines), and the remaining basins in the range following the same scheme (thin lines). Here an increasing degree of glacial modification causes a shift in the mode of the frequency distribution to lower elevations, along with an increase in the hypsometric integral, reflecting glacial modification down to lower elevations. This is the opposite trend from that seen in the Sierra Nevada and the Sangre de Cristos

Table III. Summary of Ben Ohau Range hypsometry data. Basins are listed from south to north. Mean values for hypsometric integral are: minor glaciation, 0·51; moderate glaciation, 0·49; full glaciation, 0·44

Basin	Degree of glaciation	Hypsometric integral
Darts Bush	Minor	0·523
Fraser	Minor	0·519
Dry	Minor	0·524
Gladstone	Minor	0·504
McMillan	Minor	0·534
Top McMillan	Minor	0·516
Mackenzie	Minor	0·482
Duncan	Minor	0·493
Boundary	Minor	0·501
Jacks	Moderate	0·534
Whale	Moderate	0·483
Twin	Moderate	0·492
Dead Horse	Moderate	0·485
Bush	Moderate	0·459
Freds	Full	0·466
Birch Hill	Full	0·449
Hoophorn	Full	0·394
Sawyer	Full	0·465
Black Birch	Full	0·438

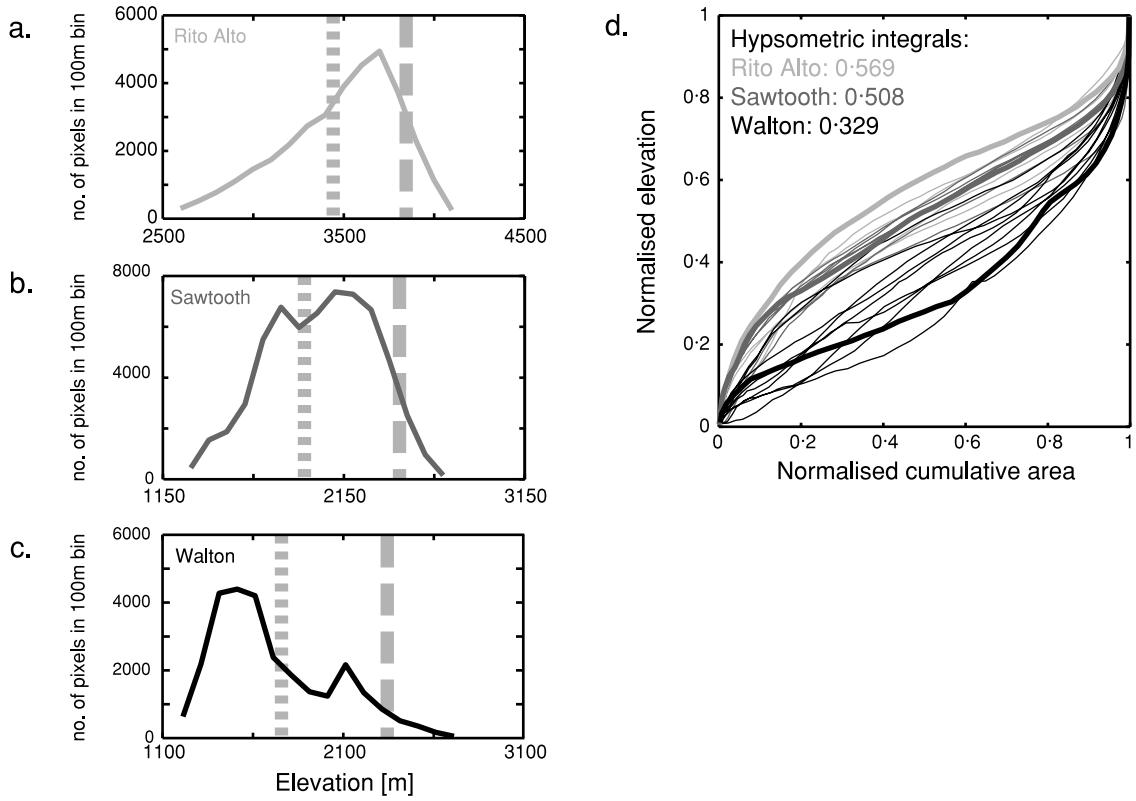

Figure 5. Comparative hypsometries from the western USA. Note varying regional ELA positions; modern (dashed, grey) and LGM (dotted, grey) for the crests of each range (from Richmond, 1965). (a) Rito Alto Creek, Sangre de Cristo Range. (b) Sawtooth Creek, Bitterroot Range. (c) Walton Creek, Glacier National Park. (d) Hypsometric curves and integrals for Rito Alto (light grey), Sawtooth (dark grey) and Walton (black) Creeks (thick lines), and other fully glaciated basins in each range following the same scheme (thin lines). Notice how the position of the ELA declining within the relief of the basin (decreasing ELA_{norm}) causes the mode of the frequency distribution to shift lower in the basin, below the LGM ELA in the case of Walton Creek. This is also reflected in a dramatic reduction in the hypsometric integral. An ELA position lower within the drainage basin relief allows much greater glacial modification of the landscape, with wide, flat valley floors developing near the basin outlet, even though this may be below the LGM ELA, particularly for large, low-gradient glaciers

distribution and the hypsometric curve (Figure 6). It is no surprise that the effect of choosing a region encompassing all of this variation in degree of glaciation has been to effectively average the variation. The overall frequency distribution is the sum of the frequency distributions of all of the basins within the range of interest, and the hypsometric curve is an 'average' of all of the hypsometric curves. A casual observer would look at Figure 6 and decide that the eastern Sierra Nevada as a whole can be described as 'partially glaciated', which is a valid interpretation, but misses the wide variety of landforms within this portion of the range. Similarly, arbitrary regions of the landscape at scales comparable to or smaller than a drainage basin can be quite unrepresentative. For example, the hypsometry of a swathe dominated by valley floors will look quite different from one dominated by ridgelines.

Importance of local circumstances

Our search for examples of unique local circumstances affecting hypsometry revealed four different situations that may be reflected in the hypsometry: icefields, hanging valleys, unusual basin shapes, and local tectonics.

As an example of the influence of an icefield, we show the hypsometry of the Waiho River (Figure 7a), which lies immediately to the south of Callery River (Figure 7b) in the Mt Cook region of the Southern Alps. The two basins have experienced similar degrees of glaciation, but a significant proportion of the Waiho Basin lies beneath the compound tributaries of the Franz Josef Glacier at high elevation. This is seen quite clearly in the

Table IV. Summary of hypsometry data for other fully glaciated basins in the western USA, as illustrated in Figure 5 (in addition to the fully glaciated basins in the Sangre de Cristos, Table II)

Basin	Range	Hypsometric integral
Lincoln	Glacier National Park	0·292
Harrison	Glacier National Park	0·408
Walton	Glacier National Park	0·329
Grinnell	Glacier National Park	0·334
Swift	Glacier National Park	0·344
Iceberg	Glacier National Park	0·364
Sprague	Glacier National Park	0·396
Snyder	Glacier National Park	0·411
Mineral	Glacier National Park	0·433
Mill	Bitterroots	0·520
Blodgett	Bitterroots	0·510
Fred Burr	Bitterroots	0·514
Sawtooth	Bitterroots	0·508
Roaring Lion	Bitterroots	0·527
Rock	Bitterroots	0·438
Tin Cup	Bitterroots	0·463

hypsometry as a peak in the frequency distribution at the very top of the basin, which is also reflected in an increase in the hypsometric integral (Figure 7c).

In Avalanche Creek in Glacier National Park (Figure 8), the two major tributaries join immediately upstream of a pronounced overdeepening. This is readily identified in the hypsometric curve of this basin in comparison with its neighbours, e.g. Snyder Creek. The hanging valleys result in a greater proportion of the valley lying at higher elevation, thus the hypsometric integral is significantly higher.

Sawmill Creek in the eastern Sierra Nevada looks much like its neighbouring partially glaciated drainage basins, with the exception that it drains into the Owens Valley through a deep canyon rather than a typical V-shaped valley. As shown in Figure 9, this difference in basin shape can be identified in the hypsometric curve, as a particularly small fraction of the drainage basin area lies at low elevations, compared with, for example, nearby Taboose Creek.

Baker Creek in the eastern Sierra Nevada (Figure 1a) traverses the fault-bounded, low-relief Coyote warp (e.g. Bateman, 1965) between the cirque at its head and the outlet into the Owens Valley (Figure 10a). This broad flat region in the upper-middle portion of the basin is reflected in both the frequency distribution of elevations, as a dramatic peak, and in the hypsometric curve, as a large proportion of the area within a narrow elevation range (Figure 10). Notice how Baker and nearby Red Mountain Creeks have quite comparable hypsometric integrals, but the shape of the hypsometric curve for Baker Creek is much flatter in the middle section. In this case it is important to note that without independent knowledge of the unique local setting of this basin, one might attribute hypsometry of this style to dramatic glacial modification, whereas glacial modification in this basin has in fact been comparatively minor.

DISCUSSION

Given the obvious distinctions between fluvial and glacial landscapes, it follows that the two should have different hypsometries. The differences in hypsometry are consistent with expectations based on studies of glacial landforms and erosion. Prior process studies have given us a good understanding of the fundamental principles of glacial erosion (e.g. Sugden and John, 1976; Benn and Evans, 1998). As temperatures fall and/or precipitation increases, causing the ELA to fall, the first stage of glaciation is the formation of a cirque glacier, and the carving of a modest overdeepening at the head of the valley. Under continuing variation in climate, glacier size fluctuates, as do the area subjected to glacial erosion, and the locus of enhanced erosion, which

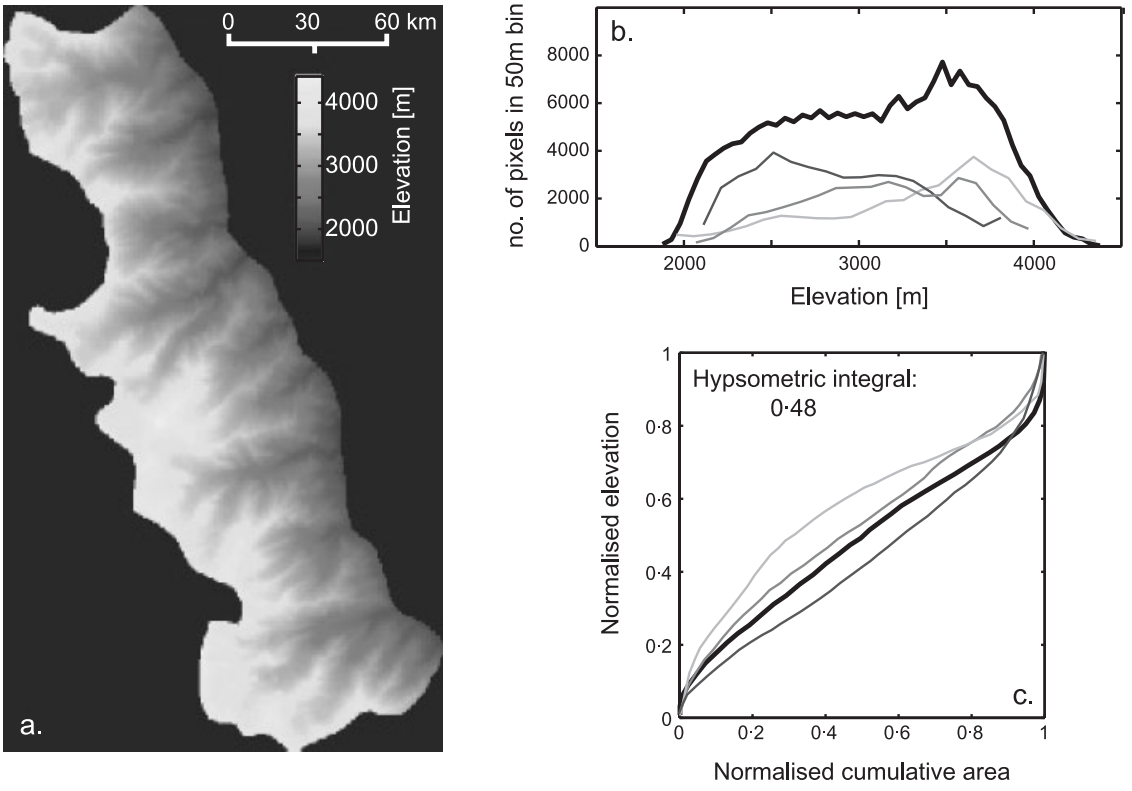

Figure 6. Hypsometry of a large portion of the study region in the eastern Sierra Nevada. (a) Digital elevation model of selected region, bounded by the drainage divide to the west and the range front to the east. Compare with Figure 1a. (b) Frequency distribution of elevations for this arbitrary region (black, bold), together with shapes (not to same scale) of frequency distributions of Inyo (dark grey, non-glacial), Bairs (medium grey, partially glaciated), and Lone Pine (light grey, fully glaciated) Creeks, taken from Figure 2a–c. (c) Hypsometric curve for this large portion of the landscape (black, bold) compared with the hypsometric curves for Inyo (dark grey), Bairs (medium grey) and Lone Pine (light grey) Creeks, from Figure 2d. Notice how the hypsometry of this large portion of the landscape effectively combines the hypsometries of the basins with varying degrees of glaciation within its boundaries, resulting in a hypsometry that looks like a 'partially glaciated' landscape

follows the ELA. If there is a sufficient increase in precipitation and/or cooling, the cirque glacier may overflow its cirque and enlarge to form a valley glacier. This valley glacier can widen the valley floor and carve steps downstream of the cirque. As the glacier continues to grow, glacial erosion will increase not merely because of the increased glacial coverage. Such large glaciers are longer-lived. Greater ice discharge, increasing velocities due to the convergence effect, and the ability to slide for a greater proportion of the melt season will result in enhanced abrasion rates, while the development of complex subglacial drainage networks may increase the effectiveness of quarrying and erosion by subglacial fluvial channels. Hence, once the ELA falls to some critical level, the glacier can scour deeply below the ELA. The research presented here demonstrates that simple topographic analyses can reveal the large-scale patterns arising from erosion under a variety of glacial conditions, in accordance with these expectations.

As shown in the eastern Sierra Nevada and the western Sangre de Cristo Range, cirque glaciers cause the mode in the frequency distribution of elevations to shift towards higher elevations; equivalently the hypsometric curve rises and the hypsometric integral increases. The mode corresponds broadly to the mean Quaternary ELA, reflecting erosion under the mean glacier size (Porter, 1989). The rise in the hypsometric curve is further accentuated by cirque glaciers bringing down ridgelines as well as valley floors (Brocklehurst and Whipple, 2002), thus decreasing the elevation range over which the hypsometric curve is normalized. As anticipated, the effect of lowering ELA within the elevation range of a basin is non-linear. Once the ELA falls to some critical level within the basin, the glacier can scour deeply below the ELA. In the Ben Ohau Range or Glacier National

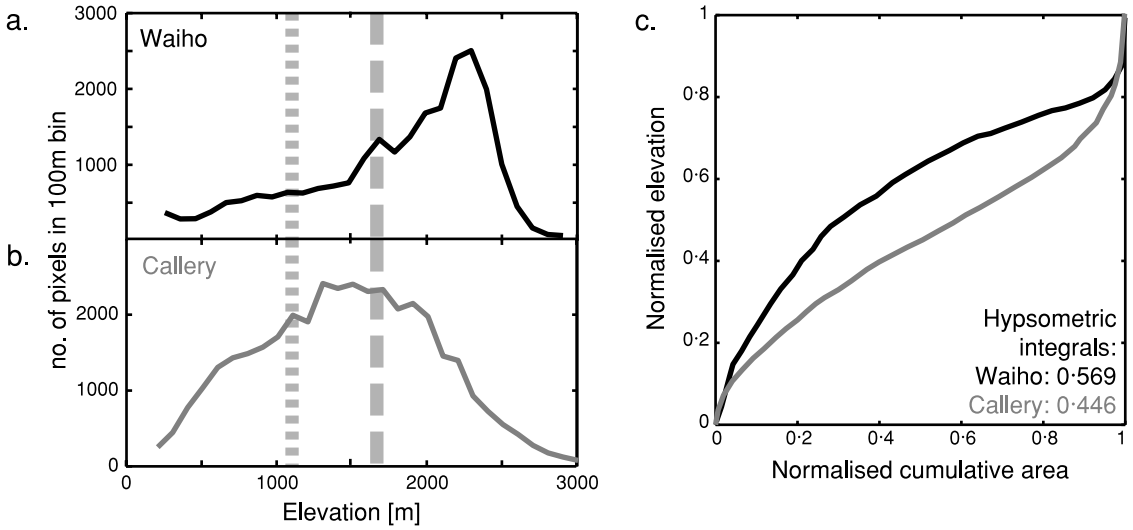

Figure 7. Hypsometry of neighbouring basins on the western side of the Southern Alps. Modern (dashed) and LGM (dotted) ELAs from Porter (1975). (a) Hypsometry of Waiho River basin. (b) Hypsometry of Callery River basin. (c) Hypsometric curve and integral for Waiho (black) and Callery (grey) River basins. The large ice cap near the range crest in the Waiho River basin introduces a large spike in the frequency distribution, also reflected in the significantly higher hypsometric integral

Park, development of larger, longer-lasting valley glaciers causes the mode to shift back towards lower elevations, and the hypsometric integral to decrease again. Comparing Figures 2d and 3d with 4d and 5d, this glacial erosion will drive the hypsometry towards, then beyond, the typical fluvial case, accentuating skewness towards low elevations and causing small hypsometric integrals, as illustrated in Figure 11a.

Within a restricted area of a given mountain range (e.g. over *c.* 50 km), only two of the three styles of hypsometric curve in Figure 11a are likely to be present. The full spectrum, from non-glaciated to large valley glaciers, requires significant gradients in either temperature or precipitation (and thus ELA), so is more likely to be seen at a considerable larger spatial range. The Ben Ohau Range comes close to having all three because of the pronounced rainshadow effect in this region, but does not exhibit any truly non-glaciated valleys. Thus there are unlikely to be circumstances where a non-glaciated basin might be confused with a glaciated basin intermediate between the cirque (high ELA) and large valley glacier (low ELA) cases, and hypsometry remains a valuable tool for examining the degree of glaciation.

The progression from landscapes featuring only modest cirque glaciers to basins dominated by large valley glaciers is somewhat reminiscent of the classic sequence of fluvial landscape evolution described by Strahler (1952). He proposed that 'young', recently uplifted, fluvially eroded landscapes have high hypsometric integrals, while increasing incision and 'maturity' result in lower hypsometric integrals as a greater proportion of the landscape is brought down to lower elevations, culminating in 'monadnock' landscapes with few peaks surrounded by extensive, low-relief regions (Figure 11b).

Hypsometry by definition attempts to describe a whole region or drainage basin with a single curve or statistic. In some cases this is desirable, and we have shown that hypsometry can be an efficient tool in assessing the impact of glaciers on a landscape. However, particular features may be lost amongst the much larger population of elevations. Within an individual basin, for example, the hypsometry will not tell you how many steps there are in the glacial longitudinal profile. Similarly, a study that combines several watersheds into larger landscape units will lose details of specific basins, but this broad-scale characterization of the landscape might be all that is necessary. Local circumstances can influence hypsometry, sometimes in quite profound ways. Hanging valleys, icefields, narrow outlet canyons and geologic structures are amongst the features of glaciated landscapes that may affect hypsometry. Thus we suggest that hypsometry should not be used in isolation when making quantitative assessments of glaciated landscapes.

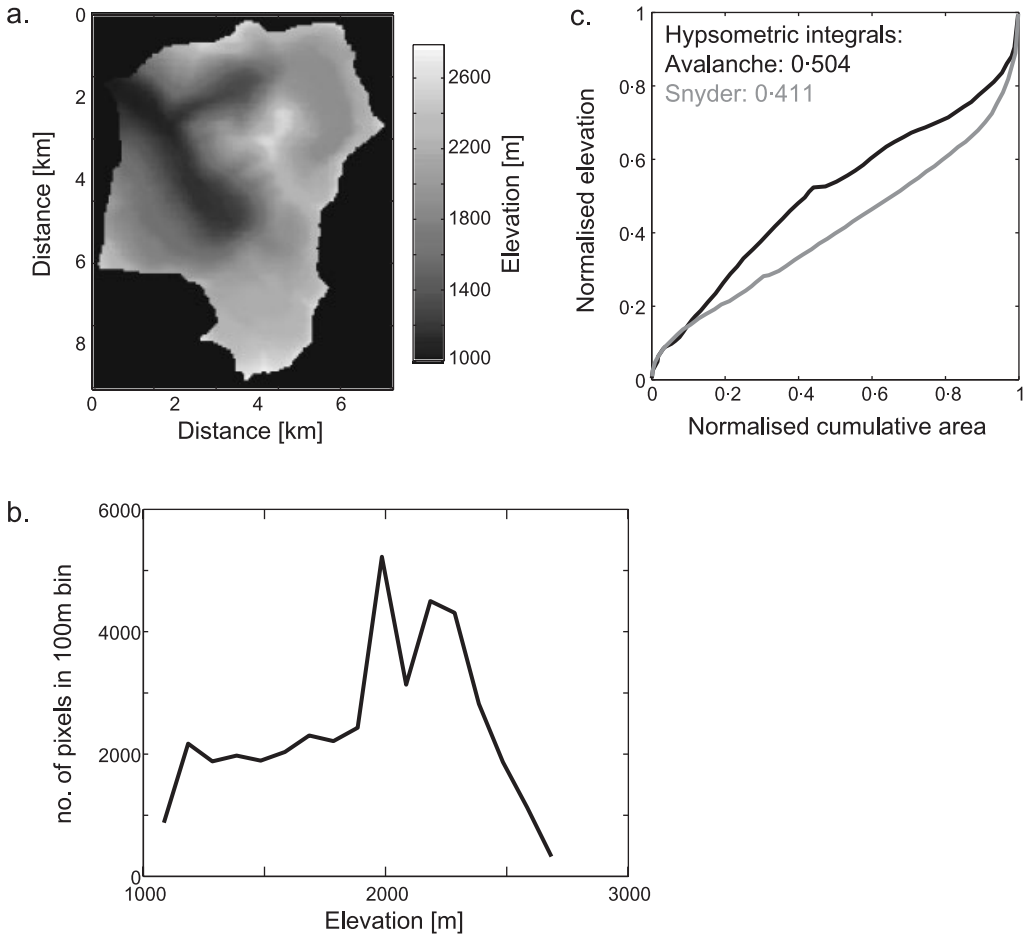

Figure 8. (a) Digital elevation model of Avalanche Creek, Glacier National Park. Notice how the two tributaries are hanging valleys above the main valley below. (b) Hypsometry of the Avalanche Creek basin. (c) Hypsometric curves for Avalanche Creek (black) and nearby Snyder Creek (grey). Notice how the presence of significant hanging valleys in Avalanche Creek causes a much greater proportion of the basin to lie at higher elevations

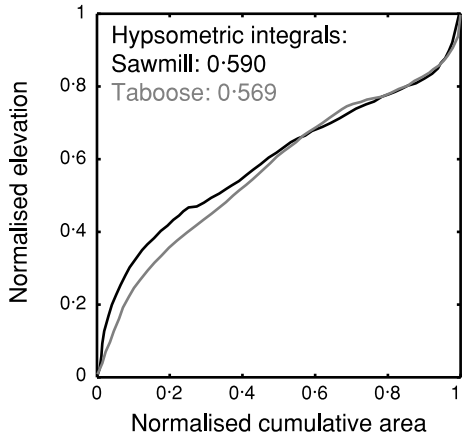

Figure 9. Hypsometric curves for Sawmill Creek (black) and Taboose Creek (grey) in the eastern Sierra Nevada (Figure 2a). Sawmill Creek enters the Owens Valley through a narrow canyon, whereas Taboose Creek has a more typical fluvial V-shaped cross-section. This is reflected in Sawmill Creek having a much smaller proportion of the basin at low elevations

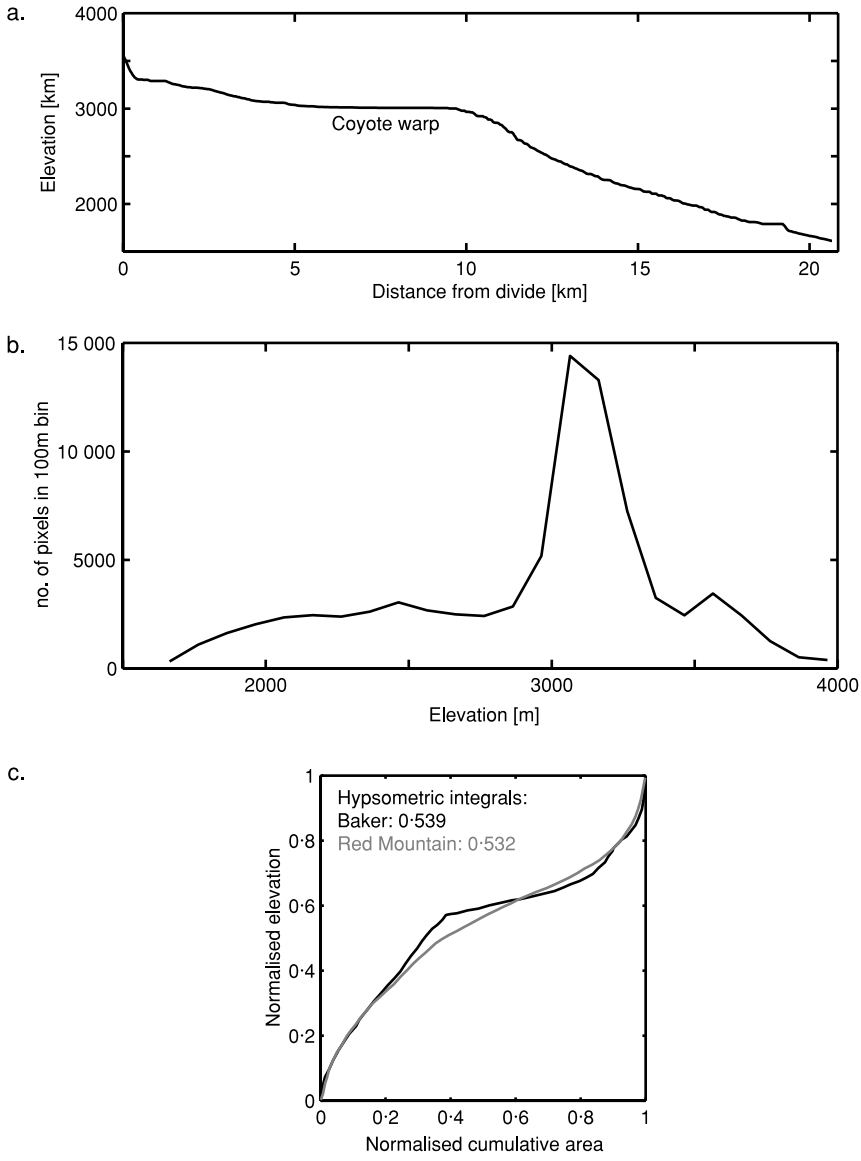

Figure 10. (a) Longitudinal profile of Baker Creek, eastern Sierra Nevada, emphasizing the low relief of the Coyote warp. (b) Frequency distribution of elevations for Baker Creek. The large spike at *c*. 3100 m reflects the large, low-relief extent of the Coyote warp, while the smaller peak at *c*. 3600 m reflects the cirque floors above this. (c) Hypsometric curves for Baker Creek (black) and nearby Red Mountain Creek (grey), which does not traverse the Coyote warp. Notice how the two are quite similar, except for the flatter section of the Baker Creek curve, which reflects the high proportion of the area within a narrow range of elevation on the Coyote warp

Kirkbride and Matthews (1997) attribute the varying amounts of glacial modification in the Ben Ohau Range to variations in time since initiation of glaciation. According to their conceptual model, the northern end of the range began rising earlier, intersected the regional ELA sooner and thus has experienced a longer period of glaciation. Furthermore ELAs are proportionally lower in the northern part of the range, so glacial modification can extend to lower in the basin. We caution that the initial condition for this landscape may have been a rising low-relief bench similar to the low-relief landscapes further to the south, in Otago (and thus looking like a miniature Altiplano in terms of hypsometry), rather than a more typical fluvially dissected landscape. Thus the landforms (as reflected in the hypsometric curve) in the southern part of the range may represent minor reworking of this landscape rather than major modification by cirque glaciers. Furthermore, for the basins at the

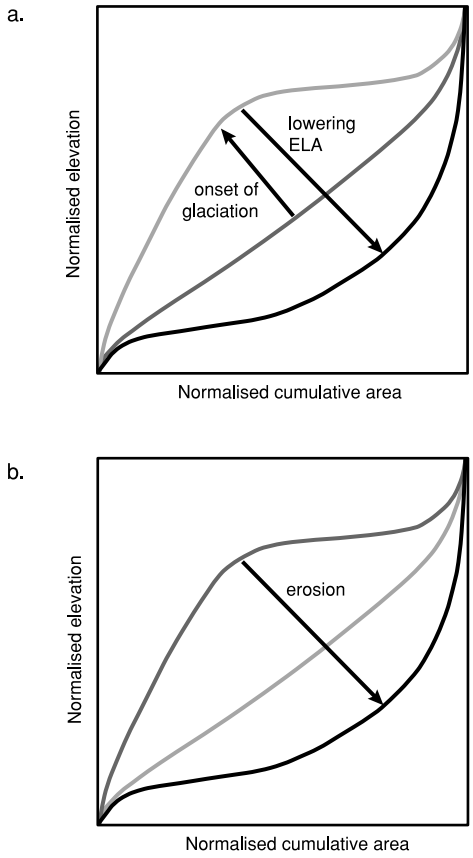

Figure 11. (a) Cartoon to illustrate effects of progressive glacial modification of an initial fluvial landscape (dark grey). Initial development of cirque glaciers associated with a high ELA will raise the hypsometric curve and integral (light grey). Lowering of the ELA and development of large valley glaciers will then lower the hypsometric curve back through its initial shape to a significantly lower position, with a correspondingly lower hypsometric integral (black). (b) Hypsometric curves for fluvial landscapes, after Strahler (1952), showing evolution from 'young' stage (light grey), through 'mature equilibrium' stage (dark grey), to 'monadnock' stage (black)

southern end to continue to evolve towards the landforms of the more northerly basins will require relative lowering of the ELA. Therefore we agree that it is the progressive northwest advection of the Ben Ohau Range into the wetter region near the Main Divide of the Southern Alps (and correspondingly lower ELAs) that is dominantly responsible for the trends in hypsometry along the range.

CONCLUSIONS

We have carried out a broad survey of the hypsometry of glaciated landscapes. Both the frequency distribution of elevations and the hypsometric curve can indicate the relative degree of glacial modification in neighbouring basins. We have identified a continuous spectrum of frequency distributions of elevations and hypsometric curves reflecting increasing modification of initially fluvial landscapes. The transition from non-glaciated to glaciated conditions, reflecting the development of cirque glaciers, tends to skew the frequency distribution to higher elevations. Further glacial modification, by substantial, long-lived valley glaciers (requiring lowering of the ELA), shifts the peak back towards lower elevations. Thus, amongst drainage basins that have been fully glaciated, the most important influence on the hypsometry is the relative position of the ELA within the drainage basin relief (measured between the basin outlet and the top of the highest peak). The transition from cirque to valley glaciers as the major influence on the landscape is reminiscent of the classic fluvial landscape development described by Strahler (1952). Given the range of different hypsometries exhibited by drainage basins with

different glaciation histories, using arbitrary regions of the landscape to determine hypsometry can mask some of the detail present in the individual drainage basins, although this approach will generally provide a good indication of the overall influence of glaciers on the landscape. Finally, unique local circumstances, such as the presence of ice-caps, major hanging valleys, narrow outlet canyons, and isolated geologic structures, can introduce major variations into the hypsometry of a glaciated landscape.

ACKNOWLEDGEMENTS

This work was supported by NSF grant EAR-9980465, NASA grant SENH99-0209-0172 (both to K.X.W.), a NASA Earth System Science Graduate Fellowship, and a CIRES Visiting Fellowship (both to S.H.B.). We would like to thank Julia Baldwin and Nicole Gasparini for their careful comments on an early version of this manuscript. Reviews by Doug Benn and Martin Kirkbride helped to clarify many of our thoughts, and are much appreciated.

REFERENCES

Andrews JT. 1972. Glacier power, mass balances, velocities and erosion potential. *Zeitschrift fur Geomorphologie N.F. Suppl. Bd.* **13**: 1–17.

Bateman PC. 1965. *Geology and Tungsten Mineralization of the Bishop District, California*. USGS Professional Paper 470, 208 pp.

Benn DI, Evans DJA. 1998. *Glaciers and Glaciation*. Arnold: London.

Blick GH, Read SAL, Hall PT. 1989. Deformation monitoring of the Ostler Fault Zone, South Island, New Zealand. *Tectonophysics* **167**: 329–339.

Braun J, Zwartz D, Tomkin JH. 1999. A new surface-processes model combining glacial and fluvial erosion. *Annals of Glaciology* **28**: 282–290.

Brocklehurst SH, Whipple KX. 2000. Hypsometry of glaciated landscapes in the western U.S. and New Zealand. *EOS* **81**: F504.

Brocklehurst SH, Whipple KX. 2002. Glacial Erosion and Relief Production in the Eastern Sierra Nevada, California. *Geomorphology* **42**: 1–24.

Brocklehurst SH, Whipple KX. In preparation. The response of glaciated landscapes to varying rock uplift rates. *Journal of Geophysical Research – Earth Surface*.

Brozovic N, Burbank DW, Meigs AJ. 1997. Climatic limits on landscape development in the northwestern Himalaya. *Science* **276**: 571–574.

Burbank DW. 1991. Late Quaternary snowline reconstructions for the southern and central Sierra Nevada, California, and a Reassessment of the 'Recess Peak Glaciation'. *Quaternary Research* **36**: 294–306.

Gillespie AR. 1982. Quaternary glaciation and tectonism in the southeastern Sierra Nevada, Inyo County, California. California Institute of Technology, Pasadena, 695 pp.

Harrison CGA, Miskell KJ, Brass GW, Saltzman ES, Sloan JL, II 1983. Continental hypsography. *Tectonics* **2**: 357–378.

Hurtrez J-E, Sol C, Lucazeau F. 1999. Effect of drainage area on hypsometry from an analysis of small-scale basins in the Siwalik Hills (Central Nepal). *Earth Surface Processes and Landforms* **24**: 799–808.

Johnson BR, Lindsey DA, Bruce RM, Soulliere SJ. 1987. *Reconnaissance geologic map of the Sangre de Cristo Wilderness Study Area, south-central Colorado*. USGS Miscellaneous Field Studies Map MF-1635-B.

Kirkbride M, Matthews D. 1997. The role of fluvial and glacial erosion in landscape evolution: the Ben Ohau Range, New Zealand. *Earth Surface Processes and Landforms* **22**: 317–327.

Lifton NA, Chase CG. 1992. Tectonic, climatic and lithologic influences on landscape fractal dimension and hypsometry: implications for landscape evolution in the San Gabriel Mountains, California. *Geomorphology* **5**: 77–114.

MacGregor KC, Anderson RS, Anderson SP, Waddington ED. 2000. Numerical simulations of glacial valley longitudinal profile evolution. *Geology* **28**: 1031–1034.

McCalpin JP. 1986. Quaternary tectonics of the Sangre de Cristo and Villa Grove Fault Zones. *Colorado Geological Survey Special Publication* **28**: 59–64.

McCalpin JP. 1987. Recurrent Quaternary normal faulting at Major Creek, Colorado: An example of youthful tectonism on the eastern boundary of the Rio Grande Rift Zone. In *Geological Society of America Centennial Field Guide – Rocky Mountain Section*, Beus SS (ed.). Geological Society of America: 353–356.

Merrand Y, Hallet B. 2000. A physically based numerical model of orogen-scale glacial erosion: Importance of subglacial hydrology and basal stress regime. *GSA Abstracts with Programs* **32**: A329.

Molnar P, England P. 1990. Late Cenozoic uplift of mountain ranges and global climate change: chicken or egg? *Nature* **346**: 29–34.

Montgomery DR, Balco G, Willett SD. 2001. Climate, tectonics and the morphology of the Andes. *Geology* **29**: 579–582.

Moore JG. 1963. *Geology of the Mount Pinchot Quadrangle, Southern Sierra Nevada, California*. USGS Bulletin 1130, 152 pp.

Moore JG. 1981. *Geologic map of the Mount Whitney Quadrangle, Inyo and Tulare Counties, California*. USGS Geologic Quadrangle Map GQ-1545.

Porter SC. 1975. Equilibrium-line altitudes of late Quaternary glaciers in the Southern Alps, New Zealand. *Quaternary Research* **5**: 27–47.

Porter SC. 1989. Some geological implications of average Quaternary glacial conditions. *Quaternary Research* **32**: 245–261.

Raymo ME, Ruddiman WF. 1992. Tectonic forcing of late Cenozoic climate. *Nature* **359**: 117–122.

Richmond GM. 1965. Glaciation of the Rocky Mountains. In *The Quaternary of the United States*, Wright HE Jr, Frey GD (eds). Princeton University Press: Princeton, NJ; 217–230.
Schumm SA. 1956. Evolution of drainage systems and slopes in badlands at Perth Amboy, New Jersey. *Geological Society of America Bulletin* **67**: 597–646.
Small EE. 1995. Hypsometric forcing of stagnant ice margins: Pleistocene valley glaciers, San Juan Mountains, Colorado. *Geomorphology* **14**: 109–121.
Small EE, Anderson RS. 1998. Pleistocene relief production in Laramide mountain ranges, western United States. *Geology* **26**: 123–126.
Spörli KB, Lillie AR. 1974. Geology of the Torlesse Supergroup in the northern Ben Ohau Range, Canterbury, New Zealand. *New Zealand Journal of Geology and Geophysics* **17**: 115–141.
Strahler AN. 1952. Hypsometric (area-altitude) analysis of erosional topography. *Geological Society of America Bulletin* **63**: 1117–1141.
Sugden DE, John BS. 1976. *Glaciers and Landscape*. Arnold: London.
Tippett JM, Kamp PJJ. 1995a. Quantitative relationships between uplift and relief parameters for the Southern Alps, New Zealand, as determined by fission track analysis. *Earth Surface Processes and Landforms* **20**: 153–175.
Tippett JM, Kamp PJJ. 1995b. Geomorphic evolution of the Southern Alps, New Zealand. *Earth Surface Processes and Landforms* **20**: 177–192.
Tomkin JH, Braun J. 2002. The influence of alpine glaciation on the relief of tectonically active mountain belts. *American Journal of Science* **302**: 169–190.
Whipple KX, Kirby E, Brocklehurst SH. 1999. Geomorphic limits to climate-induced increases in topographic relief. *Nature* **401**: 39–43.
Willgoose G, Hancock G. 1998. Revisiting the hypsometric curve as an indicator of form and process in transport-limited catchments. *Earth Surface Processes and Landforms* **23**: 611–623.

